

Topical review

High-field μ SR studies of superconducting and magnetic correlations in cuprates above T_c

J E Sonier

Department of Physics, Simon Fraser University, Burnaby, British Columbia V5A 1S6, Canada

E-mail: jsonier@sfu.ca

Abstract. The advent of high transverse-field muon spin rotation (TF- μ SR) has led to recent μ SR investigations of the magnetic-field response of cuprates above the superconducting transition temperature T_c . Here the results of such experiments on hole-doped cuprates are reviewed. Although these investigations are currently ongoing, it is clear that the effects of high field on the internal magnetic field distribution of these materials is dependent upon a competition between superconductivity and magnetism. In $\text{La}_{2-x}\text{Sr}_x\text{CuO}_4$ the response to the external field above T_c is dominated by heterogeneous spin magnetism. However, the magnetism that dominates the observed inhomogeneous line broadening below $x \sim 0.19$ is overwhelmed by the emergence of a completely different kind of magnetism in the heavily overdoped regime. The origin of the magnetism above $x \sim 0.19$ is currently unknown, but its presence hints at a competition between superconductivity and magnetism that is reminiscent of the underdoped regime. In contrast, the width of the internal field distribution of underdoped $\text{YBa}_2\text{Cu}_3\text{O}_y$ above T_c is observed to track T_c and the density of superconducting carriers. This observation suggests that the magnetic response above T_c is not dominated by electronic moments, but rather inhomogeneous fluctuating superconductivity.

PACS numbers: 74.25.Ha, 74.81.-g, 76.75.+i

1. Introduction

An applied magnetic field has been a revealing tuning parameter in the study of high- T_c cuprates. Superconducting properties can be probed via the diamagnetic response of these materials to an external magnetic field. With TF- μ SR, information on the density of the superconducting carriers can be obtained by measuring the internal magnetic field distribution of a lattice of vortices generated by an external field [1]. An applied magnetic field can also be used to partially or fully suppress superconductivity at low temperature T , to reveal competing ground states [2] and to detect normal quasiparticles [3, 4, 5, 6]. The high field required to reach the normal state of cuprates at low T is usually unattainable in a TF- μ SR experiment. Consequently, TF- μ SR studies at low T are restricted to detecting the effects of field-induced suppression of superconductivity in and around the vortex cores [7].

In recent years high TF- μ SR has found an application in the study of the magnetic response of cuprates in the normal state above T_c . It has long been believed that this region of the cuprate phase diagram holds vital clues to understanding the microscopic mechanism of high- T_c superconductivity. For example, cuprates exhibit a pseudogap at the Fermi surface above T_c [8]. There is still no consensus on the origin of the pseudogap, but establishing agreement on the specific question of whether it is associated with preformed Cooper pairs (paired electrons) or a competing phase would be a major advancement in the field. The magnetic response of cuprates above T_c became a topic of immense interest after Ong *et al* [9, 10, 11] demonstrated that a sizeable magnetic field creates a Nernst effect persisting far above T_c . The Nernst signal is accompanied by field-enhanced diamagnetism that persists in very large applied magnetic fields [12, 13]. This behaviour is qualitatively distinct from the fluctuating diamagnetism observed in conventional BCS superconductors [14], which is rapidly quenched in high fields.

The Nernst measurements accompany a growing body of experiments on high- T_c cuprates that hint at superconducting pair correlations surviving on short time and length scales far above T_c . With increasing temperature, superconductivity is ultimately destroyed by fluctuations of the pairing amplitude, fluctuations of the phase, or both. In a conventional BCS superconductor the typical energy scale of phase fluctuations is much larger than the energy gap, which in turn is proportional to T_c . Consequently, it is the vanishing of the pairing amplitude and not phase fluctuations that determines T_c . Nevertheless, just above T_c there is a critical region characterized by amplitude (Gaussian) fluctuations of short-lived Cooper pairs. The superconducting fluctuations in this region give rise to weak diamagnetism, excess specific heat, conductivity and Josephson tunneling [15].

The situation has been argued to be different in the high- T_c cuprates [16], because phase fluctuations are enhanced by the reduced dimensionality associated with superconductivity being more or less confined to the CuO_2 layers. In addition, a low density of superconducting carriers in the underdoped regime results in a reduced stiffness to phase fluctuations. These factors favour a situation where upon cooling,

bulk superconductivity is established by the onset of *long-range* phase coherence at T_c . Consequently, the simple binding of electrons into Cooper pairs may occur at temperatures well above T_c where amplitude fluctuations are still relatively weak. High-frequency conductivity measurements by Corson *et al* [17] show a residual Meissner effect in the normal state of $\text{Bi}_2\text{Sr}_2\text{CaCu}_2\text{O}_{8+\delta}$ associated with a finite phase stiffness on short time scales. Furthermore, enhanced fluctuating diamagnetism that is uncharacteristic of conventional amplitude fluctuations has been observed in several cuprates above T_c [18, 19, 20, 21, 22, 23].

The above results on cuprates have been explained in terms of a Kosterlitz-Thouless transition, below which long-range superconducting order occurs. In this model the Nernst effect is attributed to the destruction of long-range phase coherence of the Abrikosov vortex lattice (*i.e.* creation of a vortex liquid) in a two-dimensional system by thermally generated mobile vortices above the Kosterlitz-Thouless transition. This interpretation implies that there must be short-range phase coherence among Cooper pairs in sizeable regions of the sample in order to nucleate vortices. Yet the Nernst signal above T_c has also been attributed to amplitude fluctuations of short-lived Cooper pairs [24]. Pourret *et al* [25] have shown that a Nernst signal caused by amplitude fluctuations is observable in a dirty BCS superconductor far above T_c . Likewise, Rullier *et al* [26] have demonstrated that the Nernst region for $\text{YBa}_2\text{Cu}_3\text{O}_y$ is expanded by disorder above a suppressed value of T_c [26], and Bergeal *et al* [27] have provided evidence for amplitude fluctuations in cuprates above T_c from measurements of the Josephson effect in an optimally doped/underdoped junction. It is thus unclear from the experiments done thus far on cuprates whether the region above T_c is dominated by amplitude or phase fluctuations.

There is also growing evidence that the superconducting correlations in cuprates first develop in nanoscale regions at temperatures well above T_c [28, 29, 30]. Indeed, Gomes *et al* [31] have observed the development of spatially inhomogeneous pairing gaps above T_c via scanning tunnelling microscopy (STM) on $\text{Bi}_2\text{Sr}_2\text{CaCu}_2\text{O}_{8+\delta}$. With decreasing temperature the gapped regions proliferate in a way that is consistent with the eventual formation of the bulk superconducting phase below T_c via percolation or Josephson coupling of these regions. The observation of hysteresis in low-field magnetization measurements on $\text{La}_{2-x}\text{Sr}_x\text{CuO}_4$ by Panagopoulos *et al* [32] could also be interpreted as indirect evidence for fluctuating diamagnetic superconducting domains above T_c . More recently Kanigel *et al* [33] observed a Bogoliubov-like electronic dispersion in the pseudogap region of $\text{Bi}_2\text{Sr}_2\text{CaCu}_2\text{O}_{8+\delta}$, also suggestive of short-range superconducting order.

New studies of the Nernst signal in cuprates [34, 35] have now clearly distinguished the individual contributions from quasiparticles and superconducting fluctuations (phase or amplitude). The onset of a temperature dependence of the quasiparticle Nernst signal follows the doping dependence of the pseudogap temperature T^* and appears to be a consequence of developing magnetic correlations. In contrast, the vortex-like Nernst signal does not persist nearly as far above T_c .

The above experiments on cuprates suggest that for a wide doping range the region above T_c is a heterogeneous mixture of superconducting and magnetic correlations. A TF- μ SR measurement is very sensitive to the spatially inhomogeneous magnetic response of such a system, due to the local-probe nature of the positive muon (μ^+). The purpose of this review is to summarize the results of recent *high* TF- μ SR measurements on cuprates above T_c . The experiments reveal a field-induced inhomogeneous line broadening that persists far above T_c and extends from the underdoped to heavily overdoped regimes. As will be explained in this review, the dominant source of the line broadening is varied amongst the cuprates and is dependent on a competition between superconducting and magnetic correlations.

2. Transverse-field muon spin rotation (TF- μ SR)

In contrast to the closely related technique of nuclear magnetic resonance (NMR), μ SR does not rely on the Boltzmann population of spin states. Consequently, application of the μ SR method is not restricted by temperature, and an external magnetic field is not required to polarize the muon spins. In fact a powerful aspect of the μ SR technique is that it can be used to probe extremely weak internal magnetic fields in the absence of an overwhelming external field. Zero-field (ZF) μ SR has been applied extensively to cuprate systems, and has played a pivotal role in determining where magnetism occurs in the temperature versus charge doping phase diagram of these materials [36, 37, 38, 39, 40, 41, 42].

The experiments of focus in this review are transverse-field (TF) μ SR measurements, which locally probe the magnetic response of a material in the bulk. In a TF- μ SR experiment the direction of the initial muon spin polarization $\mathbf{P}(t=0)$ is oriented perpendicular to the applied magnetic field, as shown in figure 1. The muon spin precesses in the plane perpendicular to the direction of the effective local field \mathbf{B}_μ , which in general is a vector sum of the applied field, dipolar fields of nearby nuclear and atomic moments, and the Fermi contact field of spin-polarized conduction electrons at the muon site. The latter contribution is particularly important in metals, where the μ^+ is screened by conduction electrons.

In a μ SR experiment one detects the positron emitted from the decay of the implanted positive muon ($\mu^+ \rightarrow e^+ + \nu_e + \bar{\nu}_\mu$) using scintillator detectors. The light produced when a muon or positron passes through a thin plastic scintillator is transported by total internal reflection through a plastic light guide to a photomultiplier tube. Fast electronics are subsequently used to digitize, sort out, and store the electrical signals produced by the photomultiplier tubes. Each muon decay event is recorded as a function of time, resulting in a time-histogram of decay events given by

$$N_\pm(t) = N_\pm(0)e^{-t/\tau_\mu}[1 \pm a_0 G_{\text{TF}}(t) \cos(\gamma_\mu B_\mu t + \phi)], \quad (1)$$

where N_+ and N_- are the count rates of the positron detectors positioned on opposite sides of the sample, $\tau_\mu \approx 2.2 \mu\text{s}$ is the mean lifetime of the μ^+ , $a_0 \leq 1/3$ is the initial

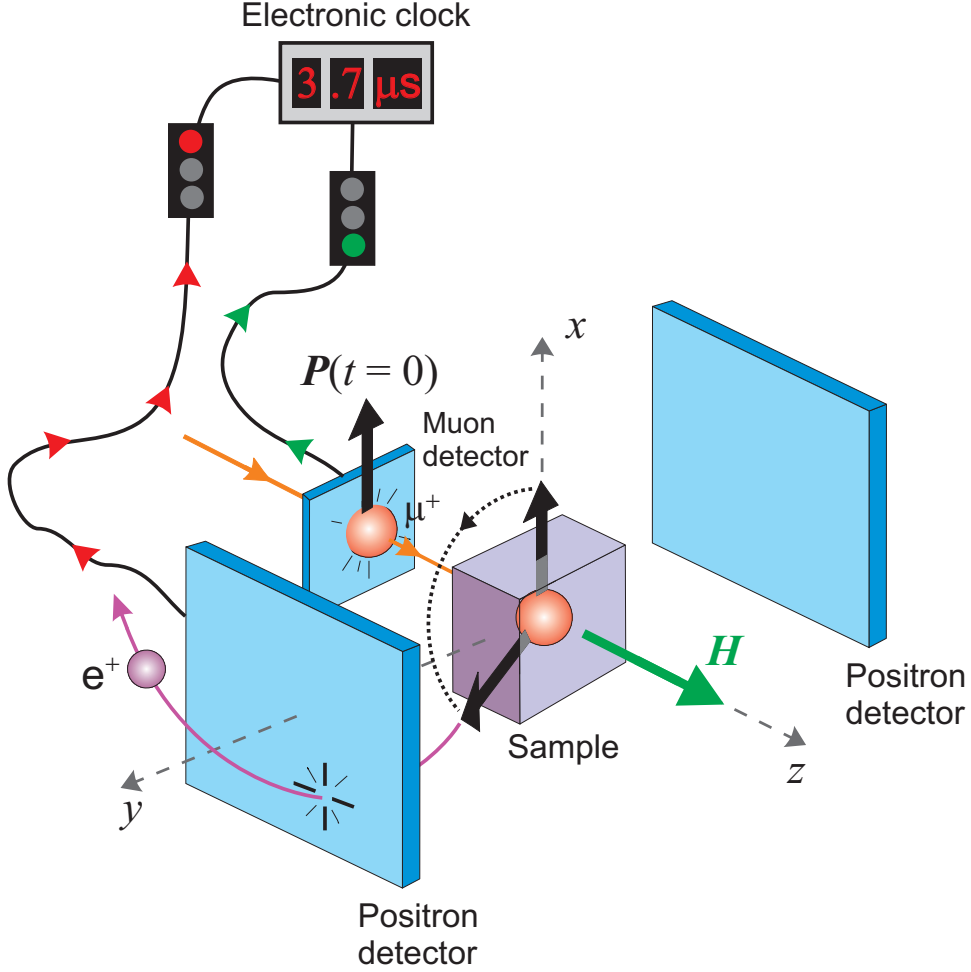


Figure 1. Basic layout of a high TF- μ SR experiment. The beam of μ^+ enters from the left with the initial muon spin polarization $\mathbf{P}(t=0)$ perpendicular to the beam momentum. The external magnetic field \mathbf{H} is applied along the beam direction, and hence perpendicular to $\mathbf{P}(t=0)$. For cuprate samples comprised of plate-like single crystals, the sample is usually mounted with the field parallel to the c -axis. This is so the larger a - b area of the crystals exposes enough of the sample to the muon beam to achieve adequate count rates. An incoming μ^+ triggers the muon detector, which starts a fast digital clock. The subsequent detection of the decay positron stops the clock. For each such decay event, the time interval is digitized and a count is added to the corresponding bin in a time histogram. Note the curved trajectory of the decay positron that occurs in a high applied field.

asymmetry (dependent on the energy of the decay positrons and numerous experimental factors), $G_{\text{TF}}(t)$ is the transverse muon spin depolarization function (further discussed below), $\gamma_\mu = 0.0852 \mu\text{s}^{-1} \text{G}^{-1}$ is the muon gyromagnetic ratio, B_μ is the magnitude of the local field, and ϕ is the (phase) angle between the axis of the positron detector and the initial muon spin polarization $\mathbf{P}(t=0)$. An example of equation (1) is shown in figure 2(a).

For a surface muon beam, where the μ^+ are generated via the decay of pions at rest in the laboratory frame of reference, the initial muon spin polarization is nearly 100 %.

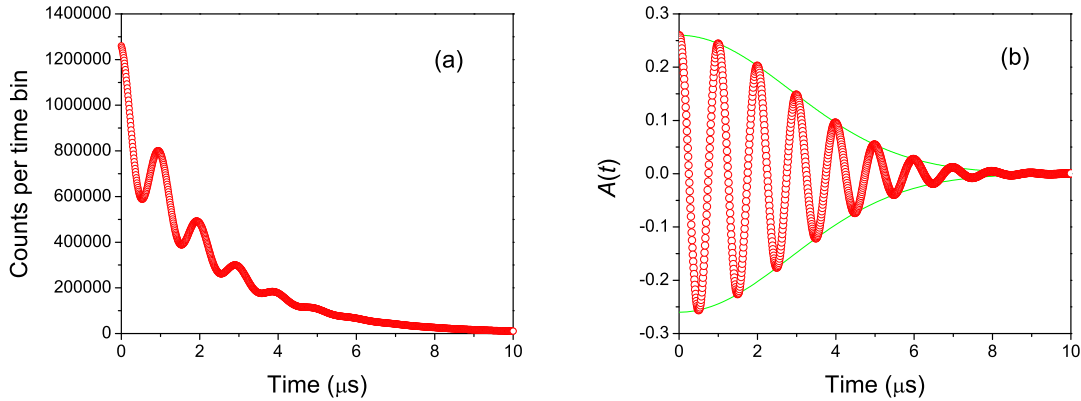


Figure 2. (a) Simulation of a raw time histogram $N(t)$ of a positron detector in a TF- μ SR experiment (*i.e.* equation (1)). The exponential decay is a consequence of the muon lifetime. The oscillation is due to the precession of the muon spins in the field, which causes the muon spin polarization to sweep past the positron detector. (b) Simulation of the corresponding asymmetry spectrum $A(t)$, as defined in equation (2). This example shows a Gaussian loss of polarization with increasing time.

This very high degree of spin polarization is one of the reasons that μ SR exceeds NMR in sensitivity to bulk magnetism. It is also important to emphasize that in contrast to the majority of the NMR active nuclei in cuprates, the spin of the muon is $1/2$, and hence the μ^+ has no quadrupole moment. Consequently, the μ^+ is a “pure” magnetic probe.

The TF- μ SR spectrum is the difference between the number of counts in the positron detectors positioned on opposite sides of the sample divided by the sum of the counts in these detectors

$$\begin{aligned} \frac{N_+ - N_-}{N_+ + N_-} &= A(t) = a_0 G_{\text{TF}}(t) \cos(\gamma_\mu B t + \phi) \\ &= a_0 P(t), \end{aligned} \quad (2)$$

where $P(t)$ is the time evolution of the muon spin polarization. More generally, $A(t)$ is referred to as the “ μ SR asymmetry spectrum”, and is analogous to an NMR free-induction decay signal. Figure 2(b) shows an asymmetry spectrum generated by equation (2). The measured TF- μ SR asymmetry spectrum has error bars that increase with time due to the muon lifetime (see figure 10).

2.1. Functional form of the depolarization

The functional form of the depolarization function $G_{\text{TF}}(t)$ is dependent on whether the effective field \mathbf{B}_μ experienced by the muon is static or fluctuating in time:

Static fields — If the muons experience an inhomogeneous distribution of dipolar fields from static nuclear or electronic moments, or the inhomogeneous field distribution created by static vortices in the superconducting state, muons stopping at different locations experience different local magnetic fields. Consequently, the muons precess with different frequencies, given by $\nu_\mu = \gamma_\mu B_\mu / 2\pi$. Over time the muon spins precessing at different frequencies dephase, causing a loss of polarization.

The host nuclei usually form a dense system of randomly oriented moments that are static on the μ SR time scale and create a Gaussian distribution of dipolar fields at the muon site. This results in a Gaussian depolarization function of the form

$$G_{\text{TF}}(t) = \exp(-\sigma^2 t^2 / 2), \quad (3)$$

where $\sigma^2 = \gamma_\mu^2 \langle B_\mu^2 \rangle$, with $\langle B_\mu^2 \rangle$ being the width of the Gaussian field distribution along the direction of the applied field. An asymmetry spectrum with a Gaussian loss of polarization is shown in figure 2(b). Barring a change in crystal structure or the onset of thermally-induced muon hopping, the depolarization rate σ associated with the nuclear moments does not depend on temperature. On the other hand, σ can depend on both the direction and strength of the applied magnetic field. In the latter situation, the nuclear moments may rapidly precess about the applied field, resulting in a reduction of σ .

A dense system of randomly frozen electronic moments will also lead to a Gaussian depolarization function. On the other hand, a dilute system of random electronic moments is described by an exponential depolarization function that corresponds to a Lorentzian distribution of internal fields [43]

$$G_{\text{TF}}(t) = \exp(-\Lambda t). \quad (4)$$

Fluctuating fields — The Gaussian depolarization observed for a dense system of static moments is modified by fluctuations. Fast fluctuations of the internal fields results in an exponential loss of the muon spin polarization, such that

$$G_{\text{TF}} = \exp(-\sigma^2 \tau t) = \exp(-\Lambda t) = \exp(-t/T_2), \quad (5)$$

where $1/\tau$ is the fluctuation rate of \mathbf{B}_μ . The exponential relaxation rate $\Lambda = \sigma^2 \tau \equiv 1/T_2$ becomes smaller as the fluctuation rate rises. This is referred to as “motional narrowing” — a term borrowed from NMR where one generally works in frequency space. It means that the width of the Fourier transform of the TF- μ SR signal is reduced as fluctuations of the local field increase.

It is not always obvious whether the exponential loss of polarization is caused by fast fluctuating internal fields or a dilute system of static moments. In these instances a longitudinal field (LF) experiment can be performed by applying a field parallel to the direction of the initial muon spin polarization. If the internal fields are static, a longitudinal field of greater magnitude will decouple the muon spin from the internal

fields and no relaxation of the LF- μ SR signal will be observed. Alternatively, fast fluctuating internal fields cause a (T_1) relaxation of the muon spin polarization parallel to the external field, by inducing transitions between the “spin up” and “spin down” Zeeman-energy eigenstates of the muon. In this case a much higher external field is needed to decouple the muon spin from the internal fields.

Disorder effects — In a system with macroscopic phase segregation, the muon will experience different local magnetic fields in the spatially-separated regions. In this case the TF- μ SR signal will be comprised of well-resolved muon precession frequencies. Moreover, the amplitudes of the different frequency components of the TF- μ SR signal, provide a direct measure of the volume fraction of each phase. Phase segregation may occur on a smaller length scale with disorder causing a spread in muon precession frequencies. Of particular interest in this review is the muon depolarization rate resulting from an inhomogeneous distribution of the magnetic susceptibility. A inhomogeneous spread $\delta\chi$ of static or time-averaged local susceptibilities χ produces a distribution of μ^+ Knight shifts $\delta K = \delta(B - H)/H$, and hence a broadening of the TF- μ SR line width [44]. It follows that

$$\delta(B - H) = \delta K H \propto \delta\chi H. \quad (6)$$

In this situation the different components of the TF- μ SR signal are numerous and cannot be isolated, but the depolarization rate of the signal is a direct measure of the width of the inhomogeneous field distribution.

2.2. Technical limitations of TF- μ SR at high magnetic field

At present the only functioning high TF- μ SR spectrometer in the world is *HiTime*, located at TRIUMF (Vancouver, Canada). The *HiTime* spectrometer utilizes a 7 T superconducting magnet, with detectors optimized for high transverse field. Several technical constraints have to be overcome to perform a TF- μ SR experiment at such high field:

(i) Surface muon beams created from pion decay at rest in the laboratory frame, result in an initial muon spin polarization that is anti-parallel to the linear momentum of the beam. A magnetic field applied perpendicular to the momentum produces a Lorentz force, which deflects the muon beam. The degree of deflection becomes problematic for fields in excess of 0.01 T. To circumvent this problem the muon spin can be rotated perpendicular to the momentum, in which case the external magnetic field may be directed parallel to the incoming beam. This can be done only on muon beam lines equipped with a “spin rotator”, which is a device consisting of crossed electric and magnetic fields.

(ii) At high fields the muon-spin precession period $T_\mu = 1/\nu_\mu = 2\pi/\gamma_\mu B_\mu$ is reduced, so that a smaller bin width must be used in the time histogram to generate the raw time

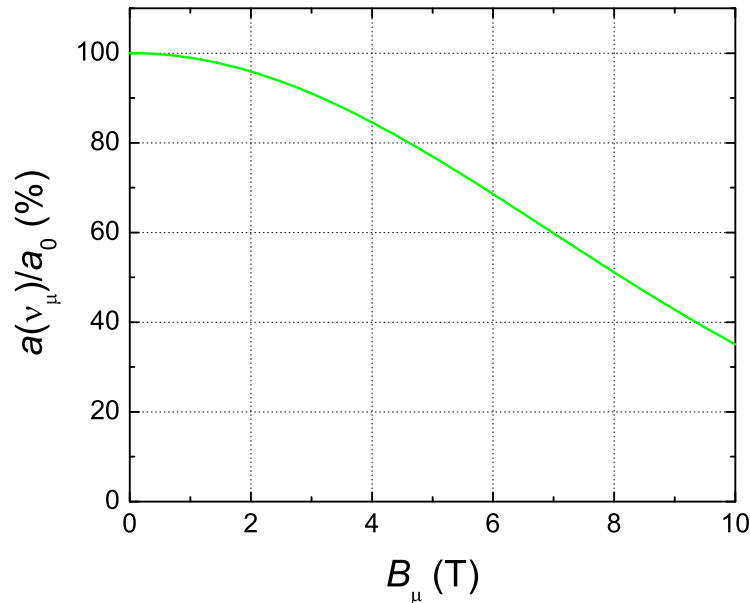


Figure 3. The amplitude of the TF- μ SR signal as a function of field for a timing resolution of 170 ps.

spectrum $N(t)$. However, the timing resolution of both the electronic circuitry and the detectors limits how small the bin width can be, and this in turn limits the maximum field measurable by TF- μ SR. With increasing magnetic field, the initial amplitude of the TF- μ SR signal decays according to [45]

$$\frac{a(\nu_\mu)}{a_0} = \exp \left[\frac{-(\pi 2.355 \nu \Delta t)^2}{4 \ln 2} \right], \quad (7)$$

where $a(\nu_\mu)$ is the amplitude of the TF- μ SR signal of precession frequency ν_μ , and Δt is the timing resolution. Figure 3 shows the field dependence of the signal amplitude of the 7 T *Hitime* spectrometer at TRIUMF, which has a time resolution of about 170 ps. At 7 T the signal amplitude is reduced to 60 % of the low-field value.

(iii) The incoming muons precess in the transverse field prior to implantation. If the field is uniform, all of the muon spins precess in phase, and the initial muon-spin polarization is preserved. However, if the field is non-uniform (*i.e.* there are field components perpendicular to the muon beam momentum), the initial polarization is reduced by de-phasing of the muon spins. Thus, high TF- μ SR experiments require superconducting magnets with good field homogeneity to be used in combination with muon beams of small cross section. Unfortunately, to preserve good timing resolution the light guides that connect the plastic scintillators to the photomultiplier tubes outside the magnet bore must be kept short to minimize attenuation and broadening of the light pulses.

This means that the cylindrical bore of the magnet must be kept short. But a short bore limits the field homogeneity of the magnet. In principle this limitation can be overcome by installing shim coils.

(iv) At high magnetic field the decay positrons undergo cyclotron motion about the applied field directed along the beam axis. The radius of the helical trajectories of the positrons is inversely proportional to the field. Hence at high field the positron detectors must be positioned closer to the sample. For surface muons that have a momentum of about 28 MeV/c, the cyclotron radius of the positrons at 7 T is only 1.3 cm. For this reason the *HiTime* spectrometer utilizes a unique compact arrangement of muon and positron counters contained within a helium-gas flow cryostat.

As a result of the above considerations, high TF- μ SR instruments are not widely available. With such limited access, high TF- μ SR experiments on cuprates (using *HiTime* at TRIUMF) have primarily focussed on the superconducting state. But in recent years such studies have shifted attention to examining the effects of high magnetic field on the normal state above T_c , and this has led to some surprising results.

3. Field-induced/enhanced magnetic order below T_c

Within the underdoped regime of cuprates, an applied magnetic field has been shown to induce static magnetic order and enhance magnetic order that is already present at $H = 0$. Demler *et al* [46] introduced a phenomenological quantum theory that describes this field-induced/enhanced effect as a competition between superconductivity and magnetic order. The original model assumes a two-dimensional (2D) system that undergoes a field-induced quantum phase transition (QPT) from a superconductor to a state of coexisting superconducting and spin-density wave (SDW) orders. In 2D, long range SDW order does not survive above $T = 0$, and hence the model strictly applies to the situation at low temperatures. The dependence of the QPT on charge-carrier concentration in the theory of Demler *et al* [46] is inline with low-temperature neutron scattering experiments on underdoped cuprates that show field-induced and/or field-enhanced SDW order in hole-doped [47, 48, 49, 50, 51] and electron-doped [52, 53] systems. Recently, Moon and Sachdev [54] have derived a microscopic theory of competing d -wave superconductivity and SDW order that reproduces the key features of the phase diagram of the phenomenological theory of Demler *et al* [46].

Field-induced/enhanced competing SDW order is also detectable by TF- μ SR, and has been observed in both hole-doped [55, 56] and electron-doped [57] systems. However, as explained above, a shortcoming of TF- μ SR is the maximum external field of 7 T that can be applied. This is particularly an issue in the $\text{YBa}_2\text{Cu}_3\text{O}_y$ family where superconductivity is more robust, and consequently higher fields are required to expose or enhance the SDW order. For example, neutron scattering experiments by Stock *et al* [58] on $\text{YBa}_2\text{Cu}_3\text{O}_{6.33}$ and $\text{YBa}_2\text{Cu}_3\text{O}_{6.35}$ show that a 6 T field directed along the c -axis is

insufficient to enhance static magnetic order via the suppression of the superconducting order parameter. Field enhanced SDW order in $\text{YBa}_2\text{Cu}_3\text{O}_{6.45}$ was recently reported by Haug *et al* [51], but an external field having a c -axis component with a magnitude of 12.5 T was used. While neutron scattering is better suited for investigations of long-range SDW order, as a local probe TF- μ SR measurements can furnish information on short-range magnetic order, disordered magnetism, and the magnetic volume fraction.

3.1. Detection of field-induced spin-glass like magnetism by μ SR

In the 2D theory of Demler *et al* [46], field-induced SDW order occurs at $T = 0$ in and around the vortex cores where superconductivity is suppressed. Long-range SDW order requires significant overlap of neighbouring vortices. The density of vortices and hence the degree of overlap increases with field. But the applicability of a 2D theory to the cuprates is limited by the significant coupling between the CuO_2 layers in the real materials. Experiments on $\text{La}_{1.90}\text{Sr}_{0.10}\text{CuO}_4$ show that the vortices [59] and the field-enhanced SDW order [60] are in fact three-dimensional (3D). Kivelson *et al* [61] have extended the phenomenological theory of Demler *et al* to the case of 3D vortices and shown that the QPT is actually to a phase in which a spatially inhomogeneous competing order coexists with superconductivity. At the QPT static magnetism is expected to develop about weakly interacting vortices, but there is no long-range static magnetic order. A crossover to long-range SDW order occurs at higher field and/or lower charge carrier concentration. The situation is summarized in figure 4.

The extended 3D model of Kivelson *et al* is supported by low-field TF- μ SR measurements, which detect static spin-glass-like (SG) magnetism in and around the vortex cores of $\text{La}_{2-x}\text{Sr}_x\text{CuO}_4$ and $\text{YBa}_2\text{Cu}_3\text{O}_y$ [62]. The static magnetism in the vortex-core region causes a suppression of the high-field ‘tail’ of the internal magnetic field distribution $n(B)$. If the distribution of the dipolar fields of the electronic moments is sufficiently broad, this is accompanied by the appearance of a low-field tail. An example of these field-induced effects are shown in figure 5 for $\text{La}_{2-x}\text{Sr}_x\text{CuO}_4$ at doping levels where static electronic moments are absent at $H = 0$. At $H < 1.5$ T the samples with $x = 0.166$ and $x = 0.176$ are in the pure SC phase depicted in the top panel of figure 4. The μ SR line shape, which is a Fourier transform of $P(t)$ and a close representation of $n(B)$, is nearly identical for these two samples. Conversely, the μ SR line shape at $x = 0.145$ shows modifications of the high-field and low-field tails expected from the emergence of SG magnetism in the vortex-core region, which places this sample in the SG+SC phase shown in figure 4. With increasing temperature the μ SR line shape at $x = 0.145$ approaches that for the higher doped samples (see figures 5(d)-(f)), and just below T_c the line shapes at the different dopings are nearly indistinguishable. This demonstrates the destruction of the static magnetism at $x = 0.145$ by thermal fluctuations. Consistent with the 3D phenomenological theory of Kivelson *et al*, the SG+SC phase deduced by TF- μ SR occurs above the hole doping concentration at which static magnetism is observed at $H = 0$ [7].

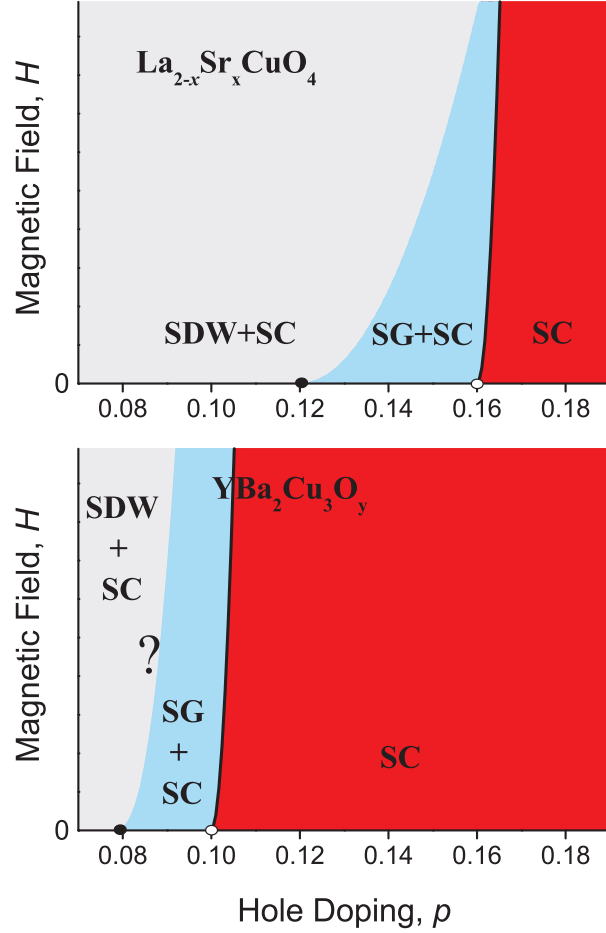


Figure 4. H -versus- p phase diagrams for $\text{La}_{2-x}\text{Sr}_x\text{CuO}_4$ and $\text{YBa}_2\text{Cu}_3\text{O}_y$ at $T = 0$. The QPT transition to a state with spin-glass-like magnetism coexisting with superconductivity (SG+SC) is deduced from low TF- μ SR measurements [62]. For $\text{La}_{2-x}\text{Sr}_x\text{CuO}_4$, neutron scattering measurements [49, 50] indicate that there is a crossover to a state where long-range static SDW order coexists with superconductivity (SDW+SC). This is also observed in $\text{YBa}_2\text{Cu}_3\text{O}_{6.45}$ [51], but the hole-doping dependence of this crossover has not yet been determined for $\text{YBa}_2\text{Cu}_3\text{O}_y$. According to Kivelson *et al* [61], the phase transition ends at an “avoided” quantum critical point (open circle). The “true” quantum critical point is at a lower hole-doping concentration (solid black circle), which apparently coincides with the critical doping at which static magnetism vanishes at $H=0$ [7].

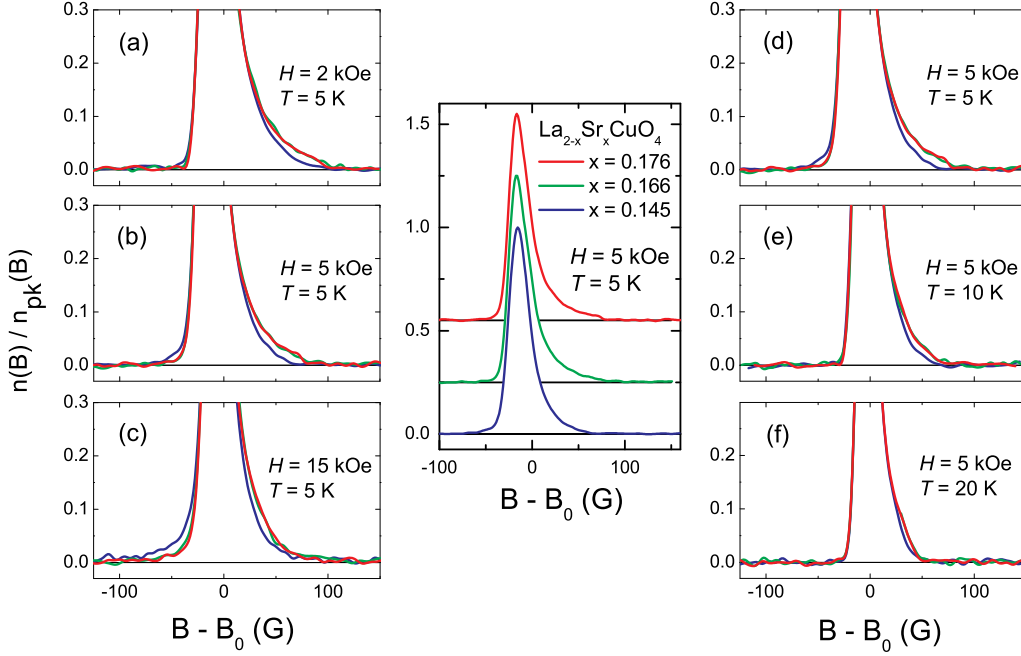


Figure 5. Doping, temperature and magnetic field dependences of the μ SR line shapes for $\text{La}_{2-x}\text{Sr}_x\text{CuO}_4$ with $x=0.145, 0.166$ and 0.176 (from Ref [62]). The center panel shows full μ SR line shapes at $H = 5$ kOe and $T = 5$ K. Panels (a)-(c) show the field dependence of the ‘tail’ regions of the normalized μ SR line shapes. Panels (d)-(f) show the temperature dependence of the ‘tail’ regions of the normalized μ SR line shapes.

3.2. Detection of field-induced static magnetic order by μ SR

As mentioned, long-range SDW order occurs in the superconducting phase (SDW+SC in figure 4) when there is a strong overlap of the vortices. A signature of strong overlap in a $d_{x^2-y^2}$ -wave superconductor is the formation of a square vortex lattice [63]. A square vortex lattice is observed in $\text{La}_{2-x}\text{Sr}_x\text{CuO}_4$ [64] at much lower fields than in $\text{YBa}_2\text{Cu}_3\text{O}_y$ [65]. This is consistent with the higher field needed to induce or enhance long-range SDW order in $\text{YBa}_2\text{Cu}_3\text{O}_y$ [51]. TF- μ SR measurements of $\text{La}_{2-x}\text{Sr}_x\text{CuO}_4$ in the SDW+SC regime show a substantial *fast* relaxing component associated with the SDW order [50, 55, 56, 66]. The fast relaxation indicates a varying degree of SDW order due to the spatial variation of the superconducting order parameter in the vortex state. The TF- μ SR measurements on $\text{La}_{2-x}\text{Sr}_x\text{CuO}_4$ show that the onset of SDW order occurs at a temperature well below T_c , whereas the neutron scattering experiments indicate that the SDW order sets in close to T_c . This difference is apparently a consequence of the different time scales of the two techniques. The theories of competing magnetic and superconducting orders do not explicitly treat the situation at finite temperature. However, thermal fluctuations are expected to cause fluctuations of the SDW order, so that static long-range SDW order exists only below T_c [54].

4. Field-induced inhomogeneous line broadening above T_c

The normal state of La-based cuprates above T_c was first studied with high TF- μ SR by Savici *et al* [55]. The TF- μ SR signals for $\text{La}_{1.88}\text{Sr}_{0.12}\text{CuO}_4$, $\text{La}_{1.875}\text{Ba}_{0.125}\text{CuO}_4$ and $\text{La}_{1.75}\text{Eu}_{0.1}\text{Sr}_{0.15}\text{CuO}_4$ exhibited a field-enhanced exponential relaxation rate that extended far above T_c . These samples all showed evidence of static electronic moments in ZF- μ SR measurements. On the other hand, no field-induced relaxation of the TF- μ SR signal was observed above T_c in optimally-doped $(\text{Bi}, \text{Pb})_2\text{Sr}_2\text{CaCu}_2\text{O}_8$, overdoped $\text{La}_{1.81}\text{Sr}_{0.19}\text{CuO}_4$ or $\text{YBa}_2(\text{Cu}_{2.979}\text{Zn}_{0.021})\text{O}_7$ samples that do not exhibit static magnetism at $H=0$. Hence the field-induced relaxation rate could be attributed to field-enhanced magnetism. However, subsequent high TF- μ SR studies have shown that this field-induced effect above T_c also takes place in $\text{La}_{2-x}\text{Sr}_x\text{CuO}_4$ samples of higher Sr (hole doping) concentration [66, 67, 68], and underdoped samples of $\text{YBa}_2\text{Cu}_3\text{O}_y$ [66], in which the electronic moments fluctuate at a rate outside the μ SR time window at $H=0$.

In the SDW+SC regime of $\text{La}_{2-x}\text{Sr}_x\text{CuO}_4$, the TF- μ SR depolarization function is observed to be of the form [55, 56, 66]

$$G_{\text{TF}}(t) = [(1 - f)e^{-\Lambda t} + fe^{-\lambda t}]e^{-\sigma^2 t^2}. \quad (8)$$

The Gaussian function accounts for the random nuclear dipole fields and is temperature independent. The two-component exponential function in square brackets implies that there are two spatially separated sources of the depolarization. A fraction f of the muons stopping in the sample sense the λ component, which is associated with SDW correlations stabilized in and around the vortex cores. The near exponential form of this depolarization is apparently a consequence of the spatial separation of the vortex cores containing short-range SDW order. In the SG+SC phase depicted in figure 4, the magnetic volume fraction associated with the spin-glass like magnetism in the vortex core region is too small to be resolved as a distinct component of the depolarization function. Thus far the λ component has been observed in underdoped $\text{La}_{1.88}\text{Sr}_{0.12}\text{CuO}_4$ [55] and $\text{La}_{1.855}\text{Sr}_{0.145}\text{CuO}_4$ [56], where the field required to induce static SDW order is attainable with high TF- μ SR. On the other hand, the exponential depolarization rate Λ of equation (8) is observed in both the underdoped and overdoped regimes of $\text{La}_{2-x}\text{Sr}_x\text{CuO}_4$. It has even been observed in heavily overdoped non-superconducting $\text{La}_{2-x}\text{Sr}_x\text{CuO}_4$ [67, 68, 69]. An analogous field-induced exponential decay of the muon spin polarization has also been detected in superconducting $\text{YBa}_2\text{Cu}_3\text{O}_y$ at $H = 7$ T [66].

As an example, figure 6 shows the temperature dependence of the exponential depolarization rates in underdoped and overdoped $\text{La}_{2-x}\text{Sr}_x\text{CuO}_4$ at $H = 7$ T. The *faster* relaxing λ component is present only in the underdoped ($x=0.145$) sample, and does not persist above T_c . This indicates that static SDW order exists at this doping and field only in the superconducting state. At both dopings the *slower* relaxing Λ component persists well above T_c . Note that in some studies a different notation is

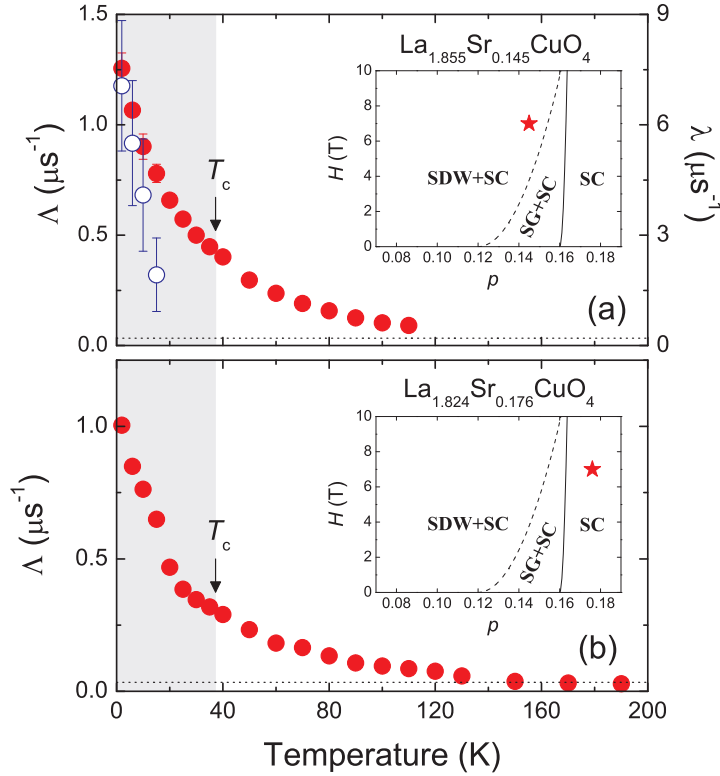


Figure 6. Temperature dependence of the exponential depolarization rates λ (open circles) and Λ (solid circles) in (a) $\text{La}_{1.855}\text{Sr}_{0.145}\text{CuO}_4$, and (b) $\text{La}_{1.824}\text{Sr}_{0.176}\text{CuO}_4$ at $H = 7$ T. The horizontal dotted lines indicate the contribution to Λ from the inhomogeneity of the external field. The bulk superconducting transition temperature at zero applied field is denoted by T_c . The inset for each panel shows the location (indicated by a star) in the H -versus- p phase diagram at $T \ll T_c$. Note the solid curves denoting the SC-to-SG+SC phase transition and the dashed curves denoting the SG+SC-to-SDW+SC crossover are approximate.

used, and the depolarization rate extending far above T_c is denoted by λ (rather than Λ). Also, at low temperatures, especially in the vortex state, the depolarization at high field is only approximately of exponential form.

4.1. Lack of dynamics

The TF- μ SR experiments measure the combined effects of static and dynamic (time-varying) local fields on the internal magnetic field distribution — meaning that both static-field inhomogeneity and fluctuating local fields may contribute to the decay rate Λ . Because μ SR can detect relaxation times below the lower limit of the NMR time window, μ SR is better suited for resolving slow fluctuations of the local field. However, it is not always easy to distinguish depolarization of the TF- μ SR signal due to an inhomogeneous static field distribution from relaxation caused by fluctuating internal

fields.

Savici *et al* [55] and MacDougall *et al* [67] have investigated the dynamics of the field-induced depolarization in $\text{La}_{2-x}\text{Sr}_x\text{CuO}_4$ above T_c by LF- μ SR. In a LF- μ SR experiment, the external field is applied parallel to the initial direction of the muon spin polarization. When the applied longitudinal field exceeds the strength of the internal static fields, any spatially inhomogeneous distribution of static field has no effect on the time evolution of the muon spin polarization. In this situation, the LF- μ SR signal is still susceptible to relaxation caused by rapidly fluctuating internal fields. When the fluctuation rate ν of the internal fields $B(t)$ is such that $\nu/\Delta \gg 1$, where Δ/γ_μ is the root mean square (rms) of $B_i(t)$ ($i = x, y, z$), the longitudinal relaxation function has an exponential decay

$$G_{\text{LF}}(t) = e^{-t/T_1}, \quad (9)$$

where $1/T_1$ is the *longitudinal* or T_1 relaxation rate given by

$$\frac{1}{T_1} = \frac{2\Delta^2/\nu}{1 + (\gamma_\mu H_z/\nu)^2}. \quad (10)$$

However, measurements on underdoped [55] and overdoped [67] $\text{La}_{2-x}\text{Sr}_x\text{CuO}_4$ show no relaxation of the LF- μ SR signal, even at temperatures far above T_c . Taking into account the accuracy of their experiment, Savici *et al* [55] set a conservative upper limit of $1/T_1 < 0.05 \mu\text{s}^{-1}$. Combined with the observation that $\Lambda \gg 1/T_1$, they have ruled out fields fluctuating at a rate greater than 10^9 Hz. Hence the field-induced relaxation rate Λ in $\text{La}_{2-x}\text{Sr}_x\text{CuO}_4$ is interpreted as a broadening of an inhomogeneous static field distribution. Likewise, LF- μ SR measurements on $\text{YBa}_2\text{Cu}_3\text{O}_{6.57}$ single crystals in fields up to $H = 5.5$ T show no evidence for dynamic relaxation [70].

4.2. Relation to the vortex-like Nernst signal

Ong *et al* [9, 10, 11] interpret the large Nernst signal they observe above T_c as being the response of a 2D vortex liquid. Like the relaxation rate Λ , the vortex-like Nernst signal decays continuously across T_c and gradually decreases with increasing temperature. However, while TF- μ SR can be used to detect the onset of a vortex solid-to-liquid transition, it is generally insensitive to variations of the vortex motion within the liquid phase itself. This is a consequence of the microsecond μ SR time scale. Upon entering the vortex liquid state, the local magnetic field distribution measured by TF- μ SR is severely narrowed by the rapid motion of the vortices [71]. Once this occurs, further increases in vortex mobility have no appreciable effect on the measured field distribution — as amply demonstrated by numerous TF- μ SR studies of vortex-liquid phases below T_c [1].

In the high TF- μ SR experiments [55, 66, 67, 68, 69], a vortex liquid is definitively ruled out as the source of Λ by the measured field dependence. Contrary to a vortex liquid, the width of the local field distribution (which is proportional to Λ) above and immediately below T_c is observed to increase with field. At the maximum field of

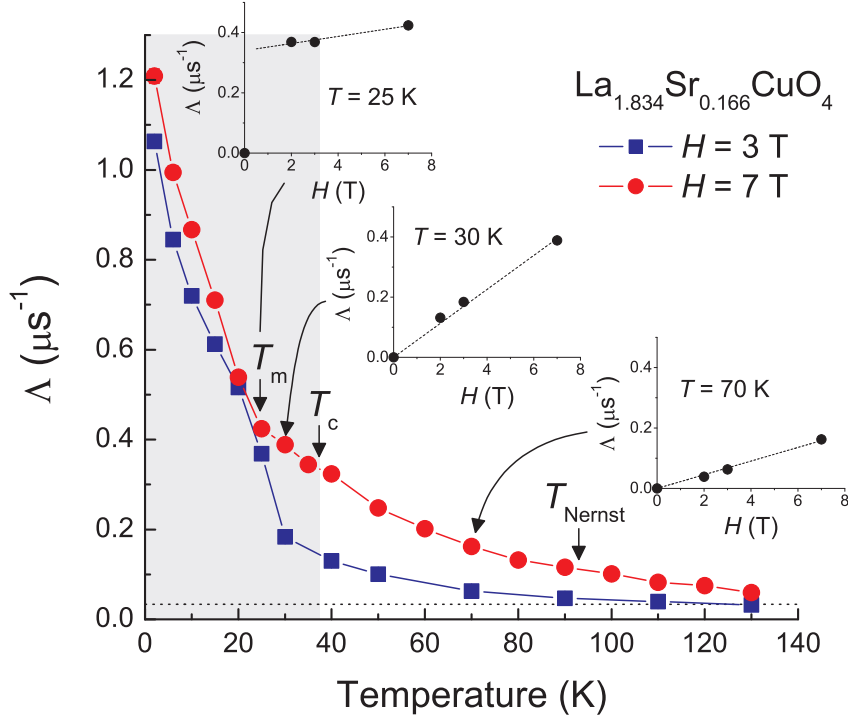


Figure 7. Temperature dependence of the exponential depolarization rate Λ in $\text{La}_{1.834}\text{Sr}_{0.166}\text{CuO}_4$ at $H = 3$ and 7 T [66]. Above T_m , Λ is proportional to H . The onset of the Nernst signal is denoted by T_{Nernst} [10], and $T_c = 37.3$ K corresponds to the bulk Λ below T_c superconducting transition temperature at $H = 0$. The horizontal dotted line indicates the contribution of the inhomogeneity of the external field to Λ .

$H = 7$ T, Λ persists above the Nernst region (see figure 7). Here it must be pointed out that the Nernst signal above T_c consists of a strongly field-dependent contribution from superconducting fluctuations, and a field-independent contribution from normal-state quasiparticles [72]. Recently Cyr-Choinière *et al* [34] have shown that the contribution due to superconducting fluctuations does not extend nearly as far above T_c as was assumed from the original experiments by Ong *et al* [9, 10, 11]. They find that in $\text{La}_{1.875}\text{Sr}_{0.125}\text{CuO}_4$, and also in $\text{La}_{2-x}\text{Sr}_x\text{CuO}_4$ doped with Eu or Nd, the Nernst signal that persists at temperatures well above the regime of superconducting fluctuations is caused by “stripe-like” charge and spin order. Similar conclusions have been reached in a Nernst study of $\text{YBa}_2\text{Cu}_3\text{O}_y$ by Daou *et al* [35], where it has also been shown that the onset of the Nernst signal coincides with the pseudogap temperature T^* .

Despite these distinctions, there does appear to be some connection between the TF- μ SR and Nernst experiments. The vortex-like Nernst signal extends into the vortex liquid state below T_c . Likewise, Λ first develops an appreciable field dependence below T_c . Figure 7 displays the temperature and magnetic field dependences of Λ for overdoped $\text{La}_{1.834}\text{Sr}_{0.166}\text{CuO}_4$. Below a temperature T_m , Λ has a weak field dependence (for fields

above the lower critical field H_{c1}) that is indicative of static disorder in a vortex glass phase [59]. At temperatures above T_m , Λ is observed to be proportional to H [55, 66, 67, 68], and this behaviour persists until Λ saturates well above T_c . It is difficult to tell from existing measurements whether the $\Lambda \propto H$ behaviour begins precisely at the onset of the vortex liquid phase below T_c . However, there is certainly a temperature range below T_c where $\Lambda \propto H$ behaviour and a vortex-like Nernst signal are simultaneously observed.

5. Variations in the hole-doping dependence

Numerous TF- μ SR studies of cuprates have been devoted to measurements of the hole-doping dependence of the depolarization rate below T_c at low field (*i.e.* in the vortex state). From such studies a universal linear relation between T_c and the muon spin depolarization rate was obtained in the underdoped regime — the so-called “Uemura plot” [73]. The depolarization rate in the vortex state is dominated by the spatial field inhomogeneity created by the arrangement of vortices, which in turn is proportional to λ_{ab}^{-2} , where λ_{ab} is the in-plane magnetic penetration depth. Because $\lambda_{ab}^{-2} \propto \rho_s$, where ρ_s is the density of superconducting carriers, the Uemura plot is considered to be a scaling relation between T_c and ρ_s .

Not much has been learned from low TF- μ SR measurements above T_c , where the muon spin depolarization rate is dominated by the nuclear dipole fields. However, the most striking and revealing aspect of recent high TF- μ SR measurements on hole-doped cuprates is the doping dependence of Λ above T_c . This turns out to be very different in the $\text{La}_{2-x}\text{Sr}_x\text{CuO}_4$ and $\text{YBa}_2\text{Cu}_3\text{O}_y$ systems.

5.1. $\text{La}_{2-x}\text{Sr}_x\text{CuO}_4$: Evidence for diverse forms of magnetism

High TF- μ SR measurements on $\text{La}_{2-x}\text{Sr}_x\text{CuO}_4$ at $H = 7$ T show a complete breakdown of the low-field Uemura relation. As shown in figure 8, the depolarization rate Λ does not track λ_{ab}^{-2} below $x \sim 0.19$ — and consequently Λ does not scale with T_c in the underdoped regime. The departure from Uemura scaling at high field is apparently caused by the slowing down of electronic moments, which fluctuate too fast at $H = 0$ to be detected by ZF- μ SR. As mentioned earlier, LF- μ SR measurements on $\text{La}_{2-x}\text{Sr}_x\text{CuO}_4$ show no evidence for spin fluctuations within the limits of detection [55, 67]. Hence according to equation (6), the $\Lambda \propto H$ behaviour observed just below and above T_c is consistent with broadening of the local field distribution by heterogeneous static magnetism. In addition, the gradual decrease of Λ with increasing temperature well above the vortex solid-to-liquid transition (see figures 6 and 7), is consistent with a gradual increase of the fluctuation rate of the electronic moments. A likely source of the line broadening is residual antiferromagnetic (AF) correlations from the parent insulator La_2CuO_4 or static SDW order [75]. At $H = 0$, neutron scattering measurements show that AF correlations persist to $x \sim 0.30$ [76]. While AF correlations fluctuate on a shorter time

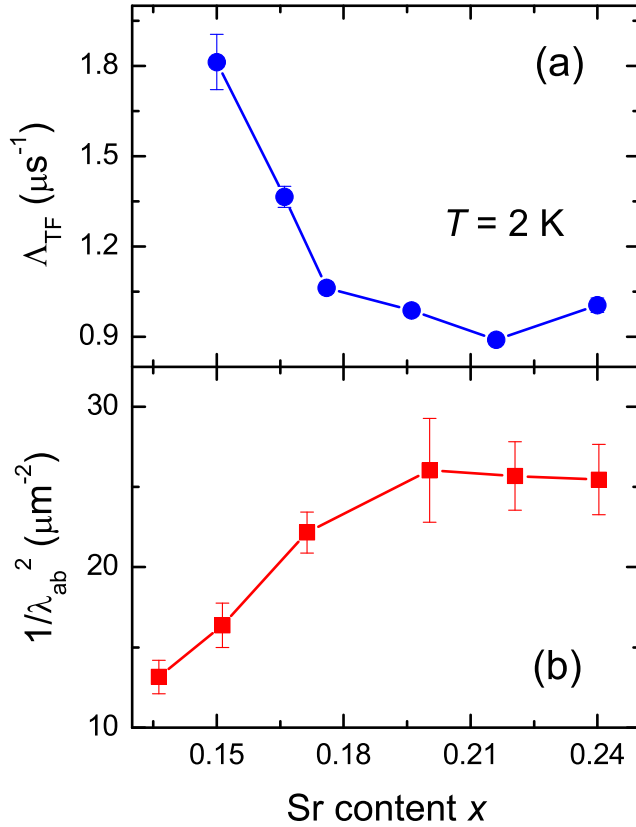


Figure 8. (a) The dependence of the muon spin depolarization rate Λ in $\text{La}_{2-x}\text{Sr}_x\text{CuO}_4$ on Sr content x (equivalent to hole-doping concentration) at $T = 2 \text{ K}$ and $H = 7 \text{ T}$. (b) The dependence of λ_{ab}^{-2} on Sr content x measured by ac susceptibility [74]

scale than the μSR time window beyond $x \sim 0.12$ [36, 37, 38], the fluctuations appear to be stabilized at high field.

As emphasized by MacDougall *et al* [68], the field-induced line broadening in $\text{La}_{2-x}\text{Sr}_x\text{CuO}_4$ is not accompanied by a sizeable shift of the average internal field. This rules out commensurate long-range order or a spatially uniform response of the sample to the external field. In other words, the high TF- μSR measurements above $x = 0.12$ are consistent with field-induced static AF order occurring in a volume fraction of the sample that decreases with increasing x . Above $x \sim 0.19$ the associated line broadening is diminished to the point that the field inhomogeneity created by the vortex lattice dominates. Consequently, Λ tracks λ_{ab}^{-2} . The observed saturation of λ_{ab}^{-2} is consistent with specific heat measurements in the superconducting state that indicate an increasing number of unpaired electrons beyond $x \sim 0.19$ [77], and magnetization measurements signifying a reduced superconducting volume fraction in the heavily overdoped regime of $\text{La}_{2-x}\text{Sr}_x\text{CuO}_4$ [78], and other cuprates [79]. Furthermore, low

TF- μ SR measurements on cuprates show a reduction of the superfluid density as the materials become progressively overdoped beyond $p \sim 0.19$ [80, 81, 82]. Together these experiments indicate that heavily overdoped cuprates are microscopically phase separated into hole-rich and hole-poor regions [83].

With increasing temperature, fluctuations reduce the line broadening associated with the AF correlations, and above T_c a new trend in the doping dependence of the line width emerges (see figure 9). Above $x \sim 0.19$, Λ is observed to increase with hole doping [68, 69]. As first reported by MacDougall *et al* [67], the width of the local field distribution above T_c continues to grow into the heavily-overdoped *non-superconducting* regime. The increase of Λ with x above $x \sim 0.19$ is concomitant with the onset of an anomalous Curie term in normal-state bulk dc magnetization measurements [84, 85, 86]. The origin of the Curie-like paramagnetism has been somewhat of a mystery. It has been proposed that phase separation and paramagnetism result from doping of holes into the Cu-3d orbital of the CuO₂ layers, rather than in the O-2p orbital [78, 86]. Doing so creates free Cu spins directly and/or by destroying the AF correlations between existing Cu spins. However, this explanation is speculative and ongoing μ SR studies are raising other possibilities.

MacDougall *et al* [68] have observed a highly anisotropic magnetic response in high TF- μ SR measurements on La_{1.70}Sr_{0.30}CuO₄. As shown in figure 10, the field-induced line broadening is significantly greater for a field applied parallel to the *c*-axis compared to the line width for a field along the *b*-axis. The anisotropy of Λ bears some resemblance to the weaker anisotropy observed in La_{1.875}Ba_{0.125}CuO₄ above T_c at $H=6$ T by Savici *et al* [55]. The anisotropy of the magnetic response in La_{1.875}Ba_{0.125}CuO₄ is almost certainly of the same origin as the anisotropy observed in bulk magnetic susceptibility measurements on La_{2-x}Sr_xCuO₄ below $x=0.19$ [87, 88]. The latter is associated with the effective susceptibility of residual AF correlations from the parent insulator [89]. Silva Neto *et al* [90] attribute the anisotropy of the magnetic susceptibility in the parent compound La₂CuO₄ to the inclusion of Dzyaloshinskii-Moriya and XY interactions in the 2D quantum Heisenberg antiferromagnet. However, it is important to stress that the width of the internal field distribution observed by high TF- μ SR increases with doping above $x \sim 0.19$, which is contrary to the diminishing contribution from residual AF correlations of the parent insulator. The high magnetic anisotropy and large value of the depolarization rate Λ (for $\mathbf{H} \parallel \mathbf{c}$) observed in heavily overdoped La_{1.70}Sr_{0.30}CuO₄ has prompted MacDougall *et al* [68] to propose that the enhanced line broadening above $x \sim 0.19$ is caused by a field-induced staggered magnetization localized about the overdoped Sr ions. However, the local spin structure cannot be directly obtained from the TF- μ SR experiments, and hence neutron scattering measurements in an applied field are needed to confirm this hypothesis.

Kopp *et al* [91] have proposed that ferromagnetic fluctuations compete with superconductivity in the overdoped regime of cuprates, and that a true ferromagnetic (FM) phase exists at $T=0$ immediately beyond the termination of the superconducting dome. Recent ZF- μ SR measurements on heavily overdoped non-superconducting

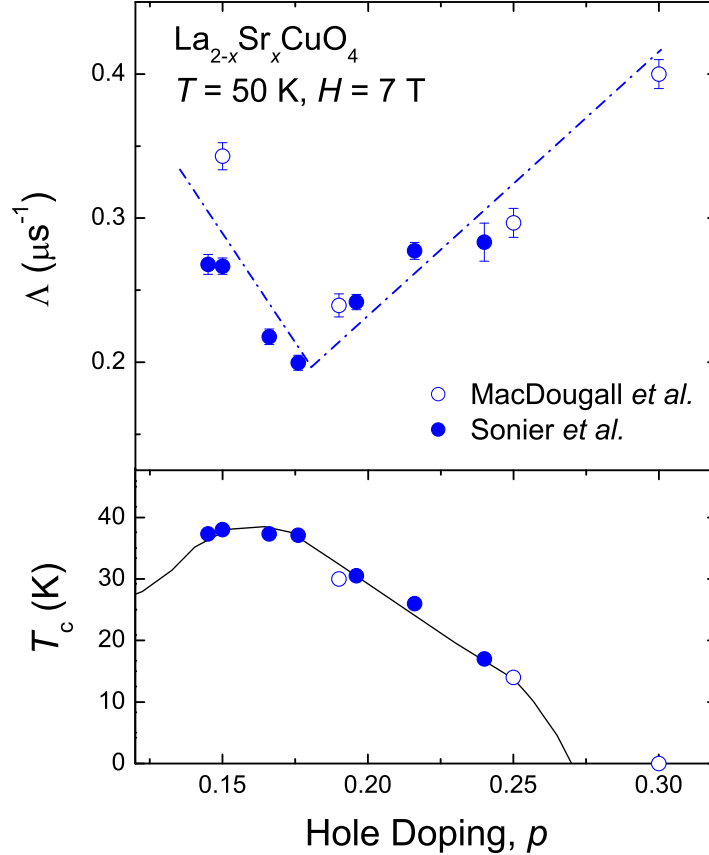


Figure 9. Hole doping dependences of Λ in $\text{La}_{2-x}\text{Sr}_x\text{CuO}_4$ at $T=50$ K and $H=7$ T (top panel), and the zero-field value of T_c (bottom panel). The open circles are data from [68] (denoted λ in the original paper). The solid circles are data from [66, 69]

$\text{La}_{1.67}\text{Sr}_{0.33}\text{CuO}_4$ single crystals show the occurrence of a frozen magnetic state below $T \sim 0.9$ K [69]. The measurements rule out the occurrence of long-range FM order, but are in accord with dilute frozen electronic moments or short-range magnetic order concentrated in dilute clusters. Consistent with the general idea of competing ferromagnetism, electronic band calculations by Barbiellini and Jarlborg [92] show that weak FM order develops about Sr-rich clusters in the heavily overdoped regime. Whether the magnetism detected by ZF- μ SR is in the form of FM clusters remains to be determined. Moreover, it is unclear at this time how the field-induced magnetism above $x \sim 0.19$ is related to the magnetism detected in $\text{La}_{1.67}\text{Sr}_{0.33}\text{CuO}_4$ at $H=0$. Interestingly, the strong magnetic anisotropy observed by MacDougall *et al.* [68] in $\text{La}_{1.70}\text{Sr}_{0.30}\text{CuO}_4$ and by others in lower-doped samples is absent in $\text{La}_{1.67}\text{Sr}_{0.33}\text{CuO}_4$ [69].

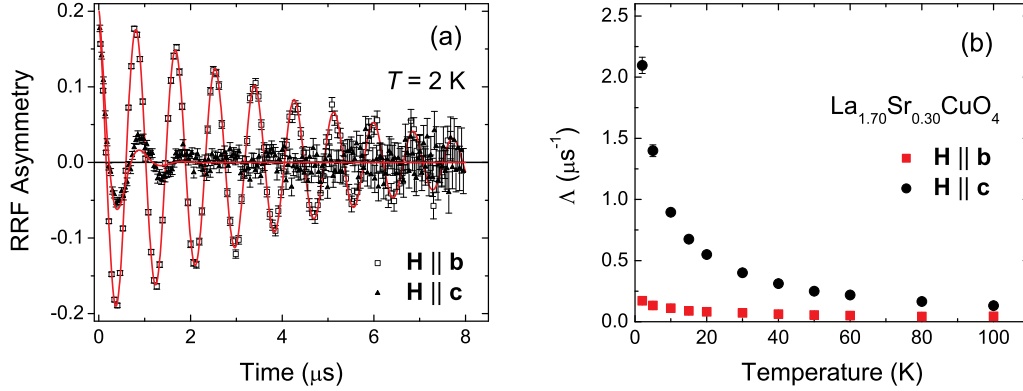


Figure 10. (a) TF- μ SR asymmetry spectra of $\text{La}_{1.70}\text{Sr}_{0.30}\text{CuO}_4$ at $T=2$ K (plotted in a rotating reference frame), for a field of $H=3$ T applied parallel to the c -axis, and parallel to the b -axis. (b) The temperature dependence of the depolarization rate Λ for the two different field orientations (from [68]).

5.2. $\text{YBa}_2\text{Cu}_3\text{O}_y$: Evidence for inhomogeneous superconducting fluctuations above T_c

Although the heavily overdoped regime cannot be reached in $\text{YBa}_2\text{Cu}_3\text{O}_y$ by oxygen doping, static magnetism at $H=0$ [39, 41, 42] occurs at a lower hole-doping concentration than in $\text{La}_{2-x}\text{Sr}_x\text{CuO}_4$. Furthermore, the maximum field of $H=7$ T in a TF- μ SR experiment is not high enough to induce long-range SDW order in $\text{YBa}_2\text{Cu}_3\text{O}_y$. Consequently, the width of the internal field distribution can be investigated over a wide range of doping where field-induced static magnetism does not necessarily dominate the muon depolarization rate.

The hole-doping dependence of Λ in the underdoped regime of $\text{YBa}_2\text{Cu}_3\text{O}_y$ has been measured at $H=7$ T by TF- μ SR [66] in samples that do not exhibit static magnetism at $H=0$. As shown in figure 11(b), Λ tracks T_c at temperatures below T_c , in agreement with the ‘‘Uemura plot’’ deduced at lower field [73]. Thus in stark contrast to underdoped $\text{La}_{2-x}\text{Sr}_x\text{CuO}_4$, the dominant contribution to Λ at high field remains the static field inhomogeneity created by vortices. Indeed the doping dependence of Λ below T_c closely resembles the doping dependence of λ_{ab}^{-2} [93]. What is most surprising is that the doping dependence of Λ continues to follow T_c and λ_{ab}^{-2} at temperatures above T_c (as shown in figure 11(c)). Moreover, the subtle suppression of Λ that is observed below T_c near a hole-doping concentration of $p=1/8$ becomes more pronounced above T_c .

In zero field, the rms deviation of the local magnetic field at the muon site increases as the hole doping concentration p is increased above $p=0$ [39, 37]. This is due to the gradual destruction of the AF phase of the parent compound. However, in both $\text{YBa}_2\text{Cu}_3\text{O}_y$ and $\text{La}_{2-x}\text{Sr}_x\text{CuO}_4$, the rms deviation of the local field vanishes deep in

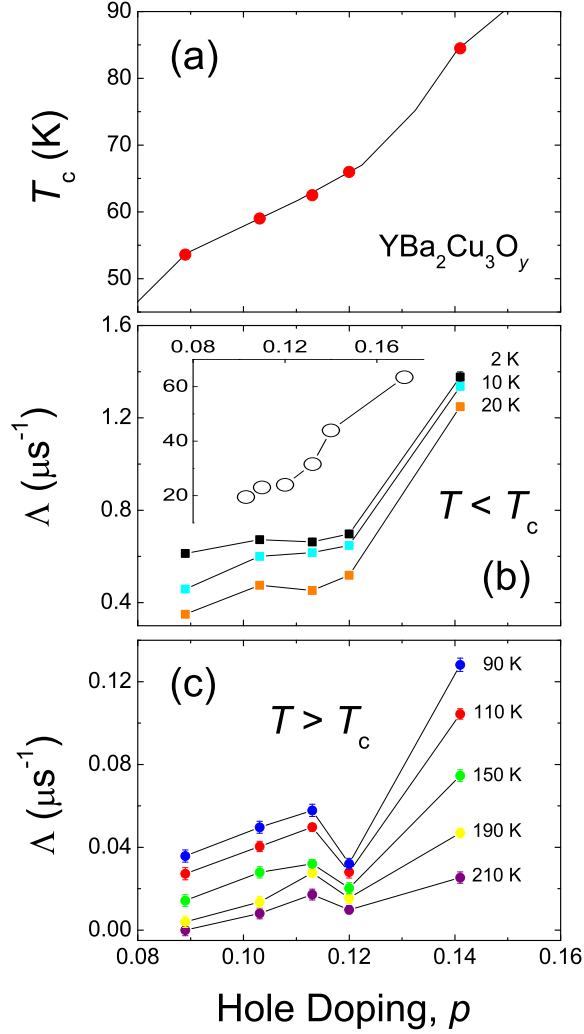


Figure 11. Hole doping dependences of (a) T_c at $H=0$, (b) Λ below T_c at $H=7$ T, and (c) Λ above T_c at $H=7$ T for $\text{YBa}_2\text{Cu}_3\text{O}_y$ (from [66]). The inset of (b) shows the hole doping dependence of $1/\lambda_{ab}^2$ (in μm^{-2}) in $\text{YBa}_2\text{Cu}_3\text{O}_y$ determined by a proper analysis of the internal field distribution of the vortex solid phase below T_c .

the underdoped regime. Moreover, in the case of $\text{La}_{2-x}\text{Sr}_x\text{CuO}_4$ there is enhanced spin freezing near $1/8$ hole doping [94], which is believed to be associated with hole and spin “stripe” ordering [95]. While this is not observed in zero-field measurements on $\text{YBa}_2\text{Cu}_3\text{O}_y$, there is a suppression of T_c in the neighbourhood of $p = 1/8$ [96]. Furthermore, Zn-doped $\text{YBa}_2\text{Cu}_3\text{O}_y$ shows an enhancement of the width of the local field distribution at $p \sim 1/8$, suggesting that there are dynamic stripes that are pinned by the Zn impurity [97]. An applied magnetic field appears to have the same effect, because the levelling off of Λ near $p = 1/8$ in figure 11(b) is consistent with a suppression of the superfluid density due to competing stripe correlations. With increasing temperature the

line width associated with the vortices decreases, and above T_c the magnetic component of the stripe order should cause an enhancement, rather than the observed suppression of Λ near $p=1/8$. This behaviour and the larger value of Λ at $p=0.141$ rules out SDW order or remnant Cu spins of the AF phase as the primary source of the field-induced line broadening above T_c .

It is clear that Λ above T_c tracks the bulk superconductivity of underdoped $\text{YBa}_2\text{Cu}_3\text{O}_y$ below T_c . One possible explanation is that Λ reflects the density of the normal state charge carriers. In other words, the applied magnetic field affects the spins of the unpaired electrons that eventually bind to form phase-coherent Cooper pairs below T_c . To have an effect on the muon depolarization rate, these electrons must localize. Yet there is no experimental evidence to support this scenario. Low-temperature thermal conductivity measurements in an external field by Sun *et al* [98] suggest that quasiparticle localization occurs, but only for $y \leq 6.50$ and not necessarily above T_c . In fact Sutherland *et al* [99] have argued that such localization does not occur even below $y=6.50$, and that the observed suppression of the thermal conductivity in a field can be explained by scattering of quasiparticles from the vortex cores.

Sanning tunneling microscopy STM measurements on $\text{Bi}_2\text{Sr}_2\text{CaCu}_2\text{O}_{8+\delta}$ by Gomes *et al* [31] indicate that superconducting-like energy gaps exist in random nanometer-size patches well above T_c , and that these regions proliferate as the sample is cooled through T_c . Assuming such spatial inhomogeneity is universal to the cuprates, the contribution of superconducting fluctuations to the Nernst signal above T_c [9, 10, 11, 34, 35] may be attributed to a vortex liquid residing in superconducting droplets above T_c . Since the doping dependence of Λ in $\text{YBa}_2\text{Cu}_3\text{O}_y$ above T_c resembles the vortex-like Nernst signal [35], it is tempting to directly associate the field-induced line broadening with the occurrence of a vortex liquid. Since TF- μ SR studies of the vortex-liquid phase of cuprates below T_c show a severely motionally-narrowed line width that decreases with increased field [1], the break up into superconducting patches appears to be the key to understanding the field-induced line broadening in $\text{YBa}_2\text{Cu}_3\text{O}_y$ above T_c . The muons will sense a unique time-averaged local diamagnetic field associated with each nanometer-size patch exhibiting fluctuating superconductivity. A distribution of such time-averaged local fields $\delta\langle B(t) \rangle$ broadens the μ SR line width according to equation (6). In this picture, each superconducting patch is characterized by a distinct local T_c that is higher than the bulk value of T_c . As the temperature is raised, an increasing number of the superconducting patches turn normal, and consequently $\delta\langle B(t) \rangle$ is reduced. This is consistent with the observed reduction of Λ in $\text{YBa}_2\text{Cu}_3\text{O}_y$ with increasing temperature.

Torque magnetometry measurements on highly-overdoped $\text{Tl}_2\text{Ba}_2\text{CuO}_{6+\delta}$ by Bergemann *et al* [100] provide insight into the field dependence of Λ at temperatures above T_c . A linear bulk diamagnetic response is observed that persists to temperatures well above T_c , which is contrary to the field dependence of a vortex liquid. This unusual result has been attributed to inhomogeneous superconductivity, whereby small regions (tens of nanometers in size) with local T_c 's much higher than the bulk T_c each exhibit a linear diamagnetic response [101]. Since the TF- μ SR line width is proportional to

an inhomogeneous distribution of time-averaged local diamagnetic susceptibilities, this model explains why Λ increases with field.

5.3. Further considerations

One may wonder why there has not been widespread reports of NMR experiments detecting a similar inhomogeneous magnetic field response in cuprates above T_c . Because the muon is a spin 1/2 particle, it is a pure local magnetic probe. In contrast, the important NMR active nuclei in the cuprates have spin greater than 1/2, and hence in addition to a magnetic dipole moment they possess an electric quadrupole moment that also couples to the local environment. Consequently, any contribution of static field inhomogeneity to the NMR line width must be separated from broadening due to electric field gradients.

Haase *et al* [102, 103] have shown that there is magnetic broadening of the ^{63}Cu and ^{17}O NMR line widths in $\text{La}_{2-x}\text{Sr}_x\text{CuO}_4$ above T_c . Like Λ in the μSR experiments, the NMR line widths in $\text{La}_{2-x}\text{Sr}_x\text{CuO}_4$ have a Curie-like dependence on temperature and are proportional to the applied field. The magnetic broadening of the NMR line width is explained by static inhomogeneity on the scale of a few lattice constants, which has been associated with non-uniform polarization of the Cu electronic moments by the external field. Furthermore, the NMR experiments by Haase *et al* reveal that the static field inhomogeneity is correlated with spatial modulations of the electric field gradients. However, the occurrence of static inhomogeneity above T_c , unrelated to sample quality (*i.e.* variations in local doping), has yet to be established by NMR in other cuprate systems. This may indicate that the normal-state μSR line width is associated with slowly fluctuating magnetism that is outside the NMR time window. But a more likely explanation is that the regions contributing to the tails of the local field distribution are too dilute to be detected by NMR. Here μSR has a distinct advantage. The nearly 100 % initial spin polarization and the large gyromagnetic ratio of the μ^+ makes μSR sensitive to regions of small volume fraction. In a dilute system the local field distribution has a Lorentzian shape, and even in the static limit this causes exponential relaxation of the TF- μSR signal. While a pure Lorentzian lineshape is unaffected by motional averaging [104], in the sample there is always a maximum local field. Thus Λ can be reduced by fluctuating internal fields, as well as a gradual disappearance of magnetic regions.

6. Conclusions

It has been explained here that the dominant contribution to the inhomogeneous field distribution detected in underdoped $\text{YBa}_2\text{Cu}_3\text{O}_y$ at high field above T_c appears to be time-averaged fields from fluctuating diamagnetic regions. The high TF- μSR measurements indicate that superconducting correlations persist to temperatures significantly above the region where a Nernst effect due to superconducting fluctuations is observed. But the inhomogeneous superconducting fluctuations detected in

$\text{YBa}_2\text{Cu}_3\text{O}_y$ by TF- μ SR are uncorrelated with the pseudogap temperature T^* , and even persist above T^* . It is important to stress that the sensitivity of the TF- μ SR line width to the fluctuating diamagnetism necessarily implies spatial inhomogeneity.

By contrast, the effect of superconducting fluctuations on the TF- μ SR depolarization rate of $\text{La}_{2-x}\text{Sr}_x\text{CuO}_4$ above T_c is masked by field-induced spin magnetism. A crossover in behaviour near $x \sim 0.19$ distinguishes remnant AF correlations of the parent insulator or SDW order from an increasing heterogeneous magnetic response in the heavily overdoped regime. The source of the heterogeneous magnetism above $x \sim 0.19$ is unknown, but its appearance in the heavily overdoped regime may explain the demise and eventual termination of superconductivity at high doping.

Acknowledgments

I would like to thank G M Luke, G J MacDougall and A T Savici for sharing and discussing their μ SR data. I would also like to thank W N Hardy, D A Bonn, R Liang, Y Ando, S Komiya, W A Atkinson, V P Pacradouni, C V Kaiser, and S A Sabok-Sayr for their contributions to some of the μ SR work discussed here. The writing of this article was supported by the Natural Science and Engineering Research Council of Canada, and the Quantum Materials program of the Canadian Institute for Advanced Research.

References

- [1] Sonier J E, Brewer J H and Kiefl R F 2000 *Rev. Mod. Phys.* **72** 769
- [2] Sachdev S 2003 *Rev. Mod. Phys.* **75** 913
- [3] Boebinger G S 1996 *Phys. Rev. Lett.* **77** 5417
- [4] Dorion-Leyraud N *et al* 2007 *Nature* **447** 565
- [5] Yelland E A *et al* *Phys. Rev. Lett.* **100** 047003
- [6] Vignolle B *et al* *Nature* **455** 952
- [7] Sonier J E 2007 *Rep. Prog. Phys.* **70** 1717
- [8] Timusk T and Statt B 1999 *Rep. Prog. Phys.* **62** 61
- [9] Xu Z A, Ong N P, Wang Y, Kakeshita T, Uchida S *Nature* **406** 486
- [10] Wang Y *et al* P 2001 *Phys. Rev. B* **64** 224519
- [11] Wang Y, Li Lu and Ong N P 2006 *Phys. Rev. B* **73** 024510
- [12] Li, L. *et al* 2005 *Europhys. Lett.* **72** 451
- [13] Wang, Y. *et al* 2005 *Phys. Rev. Lett.* **95** 247002
- [14] Bardeen J, Cooper L N and Schrieffer J R 1957 *Phys. Rev.* 108, 1175
- [15] Skocpol W J and Tinkham M 1975 *Rep. Prog. Phys.* **38** 1049
- [16] Emery V and Kivelson S A 1995 *Nature* **374** 434
- [17] Corson J, Mallozzi, Orenstein J, Eckstein J N and Bozovic I 1999 *Nature* **398** 221
- [18] Kanoda K *et al* 1988 *J. Phys. Soc. Jpn.* **57** 1554
- [19] Carballeira C, Mosqueira J, Revcolevschi R and Vidal F 2000 *Phys. Rev. Lett.* **84** 3157
- [20] Carretta P *et al* 2000 *Phys. Rev. B* **61** 12420
- [21] Lascialfari A *et al* 2002 *Phys. Rev. B* **65** 144523
- [22] Lascialfari A *et al* 2003 *Phys. Rev. B* **68** 100505(R)

- [23] Cabo L *et al* 2006 *Phys. Rev. B* **73** 184520
- [24] Ussishkin I, Sondhi S and Huse D A 2002 *Phys. Rev. Lett.* **89** 287001
- [25] Pourret A *et al* 2006 *Nature Physics* **2** 683
- [26] Rullier-Albenque F *et al* 2006 *Phys. Rev. Lett.* **96** 067002
- [27] Bergeal N *et al* 2008 *Nature Physics* **4** 608
- [28] Alvarez G, Mayr M, Moreo A and Dagotto E 2005 *Phys. Rev. B* **71** 014514
- [29] Kresin V Z, Ovchinnikov Y N and Wolf S A 2006 *Phys. Rep.* **431** 231
- [30] de Mello E V L and Dias D H N 2007 *J. Phys.: Condens. Matter* **19** 086218
- [31] Gomes, K K *et al* 2007 *Nature* **447** 569
- [32] Panagopoulos C, Majoros M, Nishizaki T and Iwasaki H 2006 *Phys. Rev. Lett.* **96** 047002
- [33] Kanigel A *et al* 2008 *Phys. Rev. Lett.* **101** 137002
- [34] Cyr-Choinière O 2009 *et al* *Nature* **458** 743
- [35] Daou R *et al* 2010 *Nature* **463** 519
- [36] Weidinger A *et al* 1989 *Phys. Rev. Lett.* **62** 102
- [37] Niedermayer Ch *et al* 1998 *Phys. Rev. Lett.* **80** 3843
- [38] Panagopoulos C *et al* 2002 *Phys. Rev. B* **66** 064501
- [39] Kiefl R F *et al* 1989 *Phys. Rev. Lett.* **63** 2136
- [40] Kanigel A *et al* 2002 *Phys. Rev. Lett.* **88** 137003
- [41] Sanna S, Allodi G, Concas G, Hillier A D and De Renzi R 2004 *Phys. Rev. Lett.* **93** 207001
- [42] Miller R I *et al* 2006 *Phys. Rev. B* **73** 144509
- [43] Walstedt R E and Walker L R 1974 *Phys. Rev.* **9** 4857
- [44] MacLaughlin D E, Bernal O O and Lukefahr H G 1996 *J. Phys.: Condens. Matter* **8** 9855
- [45] Holzschuh E 1983 *Phys. Rev. B* **27** 102
- [46] Demler E, Sachdev S and Zhang Y 2001 *Phys. Rev. Lett.* **87** 067202
- [47] Katano S, Sato M, Yamada K, Suzuki T and Fukase T 2000 *Phys. Rev. B* **62** 14677(R)
- [48] Lake B *et al* 2002 *Nature* **415** 299
- [49] Khaykovich B *et al* 2005 *Phys. Rev. B* **71** 220508(R)
- [50] Chang J *et al* 2008 *Phys. Rev. B* **78** 104525
- [51] Haug D *et al* 2009 *Phys. Rev. Lett.* **103** 017001
- [52] Matsuura M *et al* 2003 *Phys. Rev. B* **68** 144503
- [53] Kang H J *et al* 2005 *Phys. Rev. B* **71** 214512
- [54] Moon E G and Sachdev S 2009 *Phys. Rev. B* **80** 035117
- [55] Savici A T *et al* 2005 *Phys. Rev. Lett.* **95** 157001
- [56] Sonier J E 2009 *Physica B* **404** 710
- [57] Sonier J E *et al* 2003 *Phys. Rev. Lett.* **91** 147002
- [58] Stock C *et al* 2009 *Phys. Rev. B* **79** 184514
- [59] Divakar U *et al* 2004 *Phys. Rev. Lett.* **92** 237004
- [60] Lake B *et al* 2005 *Nature Materials* **4** 658
- [61] Kivelson S A, Lee D -H, Fradkin E and Oganesyan V 2002 *Phys. Rev. B* **66** 144516
- [62] Sonier J E *et al* 2007 *Phys. Rev. B* **76** 064522
- [63] Ichioka M, Hasegawa A and Machida K 1999 *Phys. Rev. B* **59** 8902
- [64] Gilardi R *et al* 2002 *Phys. Rev. Lett.* **88** 217003
- [65] Brown S P *et al* 2004 *Phys. Rev. Lett.* **92** 067004
- [66] Sonier J E *et al* 2008 *Phys. Rev. Lett.* **101** 117001
- [67] MacDougall G J *et al* 2006 *Physica B* **374-375** 211
- [68] MacDougall G J *et al* 2010 *Phys. Rev. B* **81** 014508
- [69] Sonier J E *et al* arXiv:0911.0407
- [70] Sonier J E *et al* 1998 (unpublished)
- [71] Brandt E H 1991 *Phys. Rev. Lett.* **66** 3213
- [72] Behnia K 2009 *J. Phys.: Condens. Matter* **21** 113101
- [73] Uemura Y J *et al* 1989 *Phys. Rev. Lett.* **62** 2317

- [74] Panagopoulos C *et al* 2003 *Phys. Rev. B* **67** 220502
- [75] Hinkov V 2008 *et al Science* **319** 597
- [76] Wakimoto S *et al* 2007 *Phys. Rev. Lett.* **98** 247003
- [77] Wang Y *et al* 2007 *Phys. Rev. B* **76** 064512
- [78] Tanabe Y, Adachi T, Noji T and Koike Y 2005 *J. Phys. Soc. Jpn.* **74** 2893
- [79] Wen H H *et al* 2002 *Europhys. Lett.* **57** 260
- [80] Uemura Y J *et al* 1993 *Nature* **364** 605
- [81] Niedermayer Ch 1993 *et al Phys. Rev. Lett.* **71** 1764
- [82] Bernhard C, Tallon J L, Blasius Th, Golnik A and Niedermayer Ch. 2001 *Phys. Rev. Lett.* **86** 1614
- [83] Uemura Y J *et al* 2001 *Solid State. Commun.* **120** 347
- [84] Oda M, Nakano T, Kamada Y and Ido M 1991 *Physica C* **183** 234
- [85] Nakano T *et al* 1994 *Phys. Rev. B* **49** 16000
- [86] Wakimoto S *et al* 2005 *Phys. Rev. B* **72** 064521
- [87] Terasaki I *et al* 1992 *Physica C* **193** 365
- [88] Lavrov A N, Ando Y, Komiya S and Tsukada I 2001 *Phys. Rev. Lett.* **87** 017007
- [89] Johnston D C 1989 *Phys. Rev. Lett.* **62** 957
- [90] Silva Neto M B, Benfatto L, Juricic V and Morais Smith C 2006 *Phys. Rev. B* **73** 045132
- [91] Kopp A, Ghosal A and Chakravarty S 2007 *Proc. Natl. Acad. Sci. USA* **104** 6123
- [92] Barbiellini B and Jarlborg T 2008 *Phys. Rev. Lett.* **101** 157002
- [93] Somier J E *et al* 2007 *Phys. Rev. B* **76** 134518
- [94] Julien M H 2003 *Physica B* **329-333** 693
- [95] Kivelson S A *et al* 2003 *Rev. Mod. Phys.* **75** 1201
- [96] Liang R, Bonn D A and Hardy W N 2006 *Phys. Rev. B* **73** 180505(R)
- [97] Akoshima M, Koike Y, Watanabe I and Nagamine K 2000 *Phys. Rev. B* **62** 6761
- [98] Sun X F, Segawa K and Ando Y 2004 *Phys. Rev. Lett.* **93** 107001
- [99] Sutherland M *et al* 2005 *Phys. Rev. Lett.* **94** 147004
- [100] Bergemann C *et al* 1998 *Phys. Rev. B* **57** 14387
- [101] Geshkenbein V B, Ioffe L B and Millis AJ 1998 *Phys. Rev. Lett.* **80** 5778
- [102] Haase J, Slichter C P, Stern R, Milling C T and Hinks D G 2000 *J. Supercond.* **13** 723
- [103] Haase J, Slichter C P and Milling C T 2002 *J. Supercond.* **15** 339
- [104] Silsbee R H and Hone D W 1983 *Phys. Rev. B* **27** 85